

# Formation of Al–Cr–Si quasicrystal with high silicon concentration by rapid quenching and its thermal and electrical properties

A. INOUE, H. M. KIMURA, T. MASUMOTO

*The Research Institute for Iron, Steel and Other Metals, Tohoku University, Sendai 980, Japan*

A quasicrystal revealing five-fold symmetry has been found to be formed in a rapidly quenched  $\text{Al}_{62}\text{Cr}_{19}\text{Si}_{19}$  alloy containing a large amount of metalloid silicon. From analysis by the TEM/EDX method, the quasicrystalline single phase was determined to have a composition of  $\text{Al}_{62.5}\text{Cr}_{17.6}\text{Si}_{19.9}$ . The quasicrystal is composed of randomly-oriented equiaxed grains with an average size of  $0.5\ \mu\text{m}$ . The quasicrystal transforms to a stable  $\text{Al}_{13}\text{Cr}_4\text{Si}_4$  compound with a complex cubic structure in the temperature range of 710 to 800 K. The activation energy and heat for the transformation are  $85\ \text{kJ mol}^{-1}$  and  $2.57\ \text{kJ mol}^{-1}$ , respectively. The electrical resistivities ( $\rho$ ) at 4.2 and 250 K are 2.83 and  $3.65\ \mu\Omega\text{m}$ , respectively, and its temperature coefficient at 250 K is  $9.33 \times 10^{-4}\ \text{K}^{-1}$ . The formation of the quasicrystal in the vicinity of  $\text{Al}_{13}\text{Cr}_4\text{Si}_4$  was inferred to be due to the combination effect of a great supercooling ability caused by the low melting temperature for Al–Si and Cr–Si eutectic type alloys and the difficulty of diffusivity of the constituent atoms in the ternary compound with a large unit cell and a strong bonding nature between chromium and aluminium or silicon.

## 1. Introduction

Since Schechtman *et al.* [1, 2] discovered a nonequilibrium phase (quasicrystal) with icosahedral point group symmetry, which is different from the crystalline phases with long-range period and translational order, in a rapidly quenched  $\text{Al}_{85.7}\text{Mn}_{14.3}$  alloy, a number of studies on the formation, stoichiometric alloy composition and characteristics of the quasicrystal have been carried out over the previous year. The quasicrystal has thus attracted a rapidly increasing interest as a new nonequilibrium phase which does not belong to the two categories of amorphous and conventional crystalline phases. The alloy systems in which the formation of the quasicrystalline phase in rapidly quenched alloys has been confirmed from the electron diffraction patterns revealing a distinct five-fold symmetry are as follows; Al–Mn [1, 2], Al–V [3, 4], Al–Cr [5], Al–Mn–Si [6], Mg–Al–Zn [7], Mg–Al–Cu [8], Mg–Al–Zn–Cu [9], Ti–Ni–V [10], etc. All the quasicrystals except Al–Mn–Si containing a small amount of silicon below 6 at % are composed of metallic elements and a structure model including the three-dimensional configuration of metallic atoms has been proposed [11, 12] on the basis of the above-described alloy components. This is in marked contrast to the results [13] that a number of amorphous alloys contain metalloid elements up to about 15 to 30 at % and the construction of the amorphous structure is attributed to strongly attractive interaction between metal and metalloid atoms. Very recently, the present authors have found that a quasicrystal is formed in rapidly quenched Al–Cr–Si alloys containing a metalloid (silicon) as much as about 20 at %.

This paper aims to present the alloy composition, microstructure, thermal stability and electrical property of the Al–Cr–Si quasicrystal and to compare the results of the metal–metalloid type Al–Cr–Si quasicrystal with those of metal–metal type quasicrystals such as Al–Cr [5], Al–Mn [1, 2] and Al–V [4] systems.

## 2. Experimental procedures

Al–Cr–Si alloys including a ternary compound composition  $\text{Al}_{62}\text{Cr}_{19}\text{Si}_{19}$  ( $\text{Al}_{13}\text{Cr}_4\text{Si}_4$ ) were used in the present work. The Al–Cr–Si ingots were prepared by arc melting a mixture of pure aluminium (99.99 wt %), chromium (99.75 wt %) and silicon (99.999 wt %) in a purified argon atmosphere. The compositions of alloys reported are the chemically analysed ones. Rapidly quenched ribbon specimens with about 0.02 mm thickness and about 1 mm width were prepared from the prealloyed ingots under an argon atmosphere using a single roller melt spinning apparatus. The as-quenched and annealed structures were examined by X-ray diffractometer using  $\text{CuK}\alpha$  radiation, analytical transmission electron microscopy (TEM) and differential scanning calorimetry (DSC). Thin foils for TEM were prepared by electrolytic polishing in an electrolyte of perchloric acid and ethanol with 1:9 volumetric ratio. TEM observation and microanalysis were performed on a JEM 200 CX analytical microscope equipped with a Lind energy dispersive X-ray spectrometer (EDXS) with a Model 860 analyser system for standard-less analysis of the thin films. The electron microscopy (TEM/EDXS) analysis has been known to give microchemical distribution

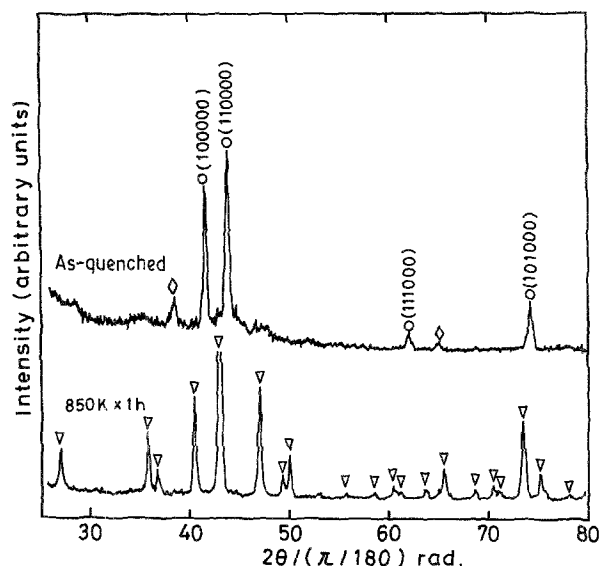


Figure 1 X-ray diffraction pattern of a rapidly quenched  $\text{Al}_{62}\text{Cr}_{19}\text{Si}_{19}$  alloy. The data of stable phase prepared by annealing the as-quenched sample at 850 K for 1 h are also shown for comparison. O, Quasicrystalline phase; ◇, aluminium phase; ▽, stable phase (cubic  $\text{Al}_{13}\text{Cr}_4\text{Si}_4$  compound).

of the constituent elements with an accuracy above about 0.5 to 1.0 at % [14], even though there are some unavoidable error factors such as surface thin film due to contamination, absorption and fluorescence effects of X-ray, limited accuracy of the standard-less analysis itself, etc. The details of the principle and technique have been described elsewhere [15]. Measurement of electrical resistivity was made by the d.c. method using the four point probe technique in a wide temperature range from 4.2. to 250 K. The temperature was measured using a calibrated germanium thermometer at temperatures below about 90 K and a calibrated diode thermometer in the higher temperature range with accuracy better than  $\pm 0.01$  K and  $\pm 0.1$  K below and above 90 K, respectively.

### 3. Results

#### 3.1. Rapidly quenched structure

Fig. 1 shows an X-ray powder-diffraction pattern as a function of diffraction angle for a rapidly quenched  $\text{Al}_{62}\text{Cr}_{19}\text{Si}_{19}$  alloy, along with the data of a stable cubic  $\text{Al}_{13}\text{Cr}_4\text{Si}_4$  compound prepared by annealing the as-quenched sample at 850 K for 1 h. Identification of the X-ray diffraction peaks corresponding to the quasicrystal with an icosahedral structure was made by using six independent Miller indices as proposed by Bancel *et al.* [16]. As indexed in Fig. 1, the diffraction pattern of the  $\text{Al}_{62}\text{Cr}_{19}\text{Si}_{19}$  alloy consists mainly of quasicrystalline phase. The deviation of chromium and silicon concentrations from  $\text{Al}_{62}\text{Cr}_{19}\text{Si}_{19}$  was confirmed to result in an increase in the diffraction intensities of the second phase. Accordingly, the X-ray data allow us to conclude that a mostly single phase with quasicrystal structure is formed in the vicinity of 19 at % Cr and 19 at % Si.

Table I summarizes the interlattice spacings of the quasicrystalline phase in a rapidly quenched  $\text{Al}_{62}\text{Cr}_{19}\text{Si}_{19}$  alloy together with the data for the quasicrystalline  $\text{Al}_{84.6}\text{Cr}_{15.4}$  alloy. Here it is important to

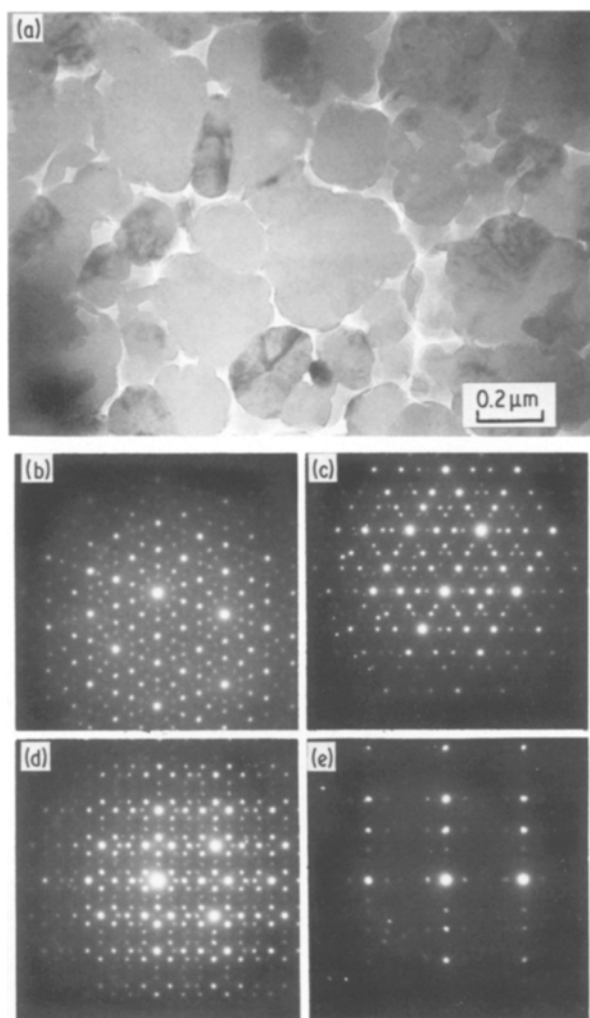


Figure 2 (a) Bright-field electron micrograph and (b-e) selected area diffraction patterns of a rapidly quenched  $\text{Al}_{62}\text{Cr}_{19}\text{Si}_{19}$  alloy.

point out that the interlattice spacing of Al-Cr-Si quasicrystal is slightly smaller than that of  $\text{Al}_{84.6}\text{Cr}_{15.4}$  quasicrystal, probably because of a decrease in aluminium content with a larger atomic size.

Fig. 2a shows a bright-field electron micrograph, and (b-e) selected area diffraction patterns of rapidly quenched  $\text{Al}_{62}\text{Cr}_{19}\text{Si}_{19}$  alloy. The selected area diffraction patterns can be indexed as  $[100000]_q$ ,  $[111000]_q$ ,  $[110000]_q$  and  $[112000]_q$ . These patterns reveal five-fold, three-fold and two-fold symmetries, the same as those of rapidly quenched  $\text{Al}_{85.7}\text{Mn}_{14.3}$  alloy reported by Schechtman *et al.* [1]. The bright-field image shown in Fig. 2a reveals that the quasicrystalline phase consists of spherulitic grains with a size of about  $0.5 \mu\text{m}$ , and one cannot see radiating branches stemming from a central core, which

TABLE I Analysis of X-ray diffraction pattern of the quasicrystalline phase in a rapidly quenched  $\text{Al}_{62}\text{Cr}_{19}\text{Si}_{19}$  alloy. The data of  $\text{Al}_{84.6}\text{Cr}_{15.4}$  quasicrystal are also presented for comparison

Index	Interlattice spacing (nm)	
	$\text{Al}_{62}\text{Cr}_{19}\text{Si}_{19}$	$\text{Al}_{84.6}\text{Cr}_{15.4}$
(100000)	0.2184	0.2199
(110000)	0.2070	0.2088
(111000)	0.1498	0.1515
(101000)	0.1280	0.1293

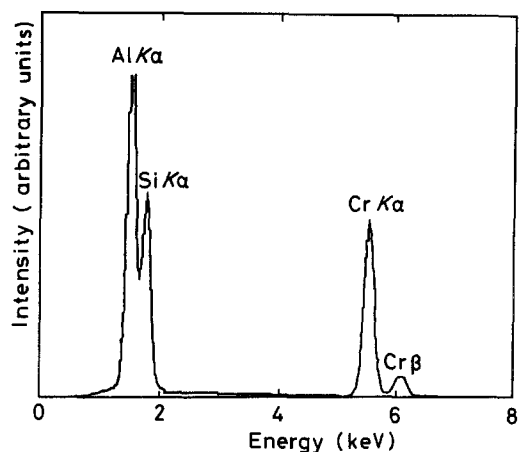


Figure 3 Energy dispersive X-ray spectra of a rapidly quenched  $\text{Al}_{62}\text{Cr}_{19}\text{Si}_{19}$  alloy.

were observed for Al–Mn [1, 2], Al–V [3, 4] and Al–Cr [5] quasicrystals.

The analytical compositions of the quasicrystalline phase were examined by the EDX method from a limited region smaller than about 5 nm in a rapidly quenched  $\text{Al}_{62}\text{Cr}_{19}\text{Si}_{19}$  alloy. A typical example of the EDX spectrum taken from the quasicrystal spherulite in  $\text{Al}_{62}\text{Cr}_{19}\text{Si}_{19}$  alloy is presented in Fig. 3. The average chromium and silicon concentrations in the quasicrystalline phase were analysed to be about 17.6 at % and about 19.9 at %. The analytical values are nearly the same as the nominal alloy composition. Furthermore, we obtained a preliminary result that no systematic variation in analytical chromium and silicon concentrations in the quasicrystal with nominal chromium and silicon contents is seen for the Al–Cr–Si alloys. From these results, the nonequilibrium quasicrystal is concluded to have a limited stoichiometric composition of  $\text{Al}_{13}\text{Cr}_4\text{Si}_4$ . This is in good contrast to the previous results [4, 5] that the quasicrystalline phase in Al–Mn, Al–V and Al–Cr systems has analytical solute concentrations ranging from 17.0 to 23.6 at % Mn, 18.9 to 20.4 at % V and 9.0 to 15.4 at % Cr.

It has very recently been proposed [11, 17] from high-resolution electron microscopic images of the quasicrystalline  $\text{Al}_{85.7}\text{Mn}_{14.3}$  and  $\text{Al}_{80}\text{Mn}_{20}$  phases that the quasicrystalline phase is composed of two types of basic golden rhombohedra, acute and obtuse ones, consisting of aluminium and manganese atoms. It has furthermore been reconfirmed that a chemical formula of the Al–Mn quasicrystal determined from analysed compositions is consistent with the atomic ratio of manganese to aluminium in the structure model [11, 12] including the three-dimensional configuration of aluminium and manganese atoms in the icosahedral quasicrystals. The total concentration of chromium and silicon atoms excluding aluminium reaches as much as about 38 at % which is much higher than the solute concentration (16 to 22.5 at %) for Al–Mn quasicrystals. Furthermore, the metalloid (silicon) concentration is also much higher as compared with  $\text{Al}_{74}\text{Mn}_{20}\text{Si}_6$  alloy [6] which is only an alloy containing silicon among the quasicrystal alloys reported up to date. The marked difference in the alloy

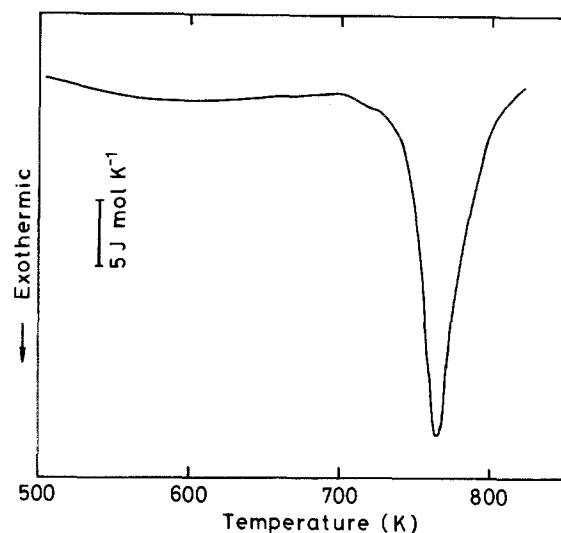


Figure 4 Differential scanning calorimetry curve of a quasicrystalline  $\text{Al}_{62}\text{Cr}_{19}\text{Si}_{19}$  alloy.  $\Delta H_f = 1160 \text{ J mol}^{-1}$ .

composition suggests that the structure model proposed for the Al–Mn quasicrystal is not always appropriate for the present Al–Cr–Si alloys containing chromium and silicon atoms as much as about 38 at %. A new three-dimensional structure model including a site of silicon metalloid is desired to be constructed for the Al–Cr–Si quasicrystal.

### 3.2. Thermal properties

Fig. 4 shows the DSC curve obtained at a heating rate of  $40 \text{ K min}^{-1}$  for a quasicrystalline  $\text{Al}_{62}\text{Cr}_{19}\text{Si}_{19}$  alloy. A high intensity exothermic peak resulting from the transformation of quasicrystal to cubic  $\text{Al}_{62}\text{Cr}_{19}\text{Si}_{19}$  compound is seen in the temperature range from 710 to 800 K, suggesting that the structural change starts at about 710 K and is complete in a relatively narrow temperature range of about 90 K. The exothermic heat by the structural change was estimated to be  $2.57 \text{ kJ mol}^{-1}$ , being considerably larger than  $180 \text{ J mol}^{-1}$  for  $\text{Al}_{80}\text{Mn}_{20}$  [18],  $870 \text{ J mol}^{-1}$  for  $\text{Al}_{82.5}\text{V}_{17.5}$  [19] and  $550 \text{ J mol}^{-1}$  for  $\text{Al}_{84.6}\text{Cr}_{15.4}$  [5] with quasicrystalline phase, suggesting that the dissolution of silicon significantly increases the thermal stability of quasicrystal.

The activation energy for the transformation from quasicrystal to stable compound was determined from the change of the exothermic peak temperature on the DSC curve with heating rate by the Kissinger method [20]. As shown in Fig. 5, a linear relationship exists between  $\ln(\alpha/T_p^2)$  and  $1/T_p$ , where  $\alpha$  is the heating rate and  $T_p$  the temperature of the exothermic peak. The activation energy is estimated to be about  $85 \text{ kJ mol}^{-1}$ . It is reasonable to consider that the transformation of the nonequilibrium quasicrystalline phase occurs by a nucleation and growth process which is controlled by the diffusion of aluminium, chromium and/or silicon atoms. The activation energy for diffusion in crystalline aluminium has been reported [21] to be  $142 \text{ kJ mol}^{-1}$  at temperatures ranging from 729 to 916 K for aluminium,  $252 \text{ kJ mol}^{-1}$  at temperatures ranging from 859 to 922 K for chromium and  $124 \text{ kJ mol}^{-1}$  at temperatures ranging from 617 to 904 K for silicon. The activation energy for the transformation of the Al–Cr–Si quasicrystal is considerably smaller than

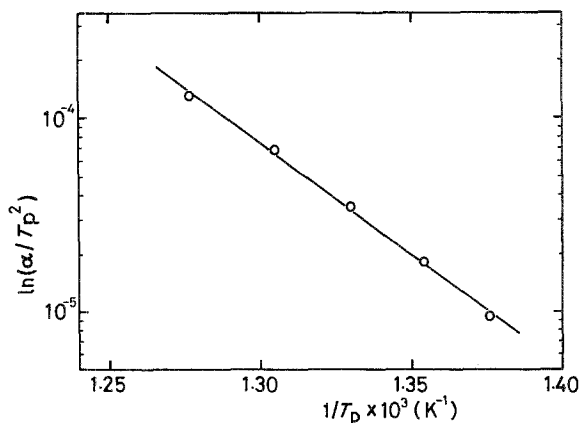


Figure 5 Kissinger plots of  $\ln(\alpha/T_p^2)$  against  $1/T_p$  for a quasicrystalline  $\text{Al}_{62}\text{Cr}_{19}\text{Si}_{19}$  alloy.

those of aluminium, chromium or silicon in aluminium crystal, indicating that the diffusion of the constituent atoms in the Al–Cr–Si quasicrystal is easier as compared with aluminium crystal. This ease is thought to be due to the result that the quasicrystal has a higher configuration energy of the constituent atoms and hence the long-range diffusivity of their atoms is significantly enhanced.

In order to assess the change in the thermal energy state of the quasicrystal upon heating up to a temperature below the onset transformation temperature 710 K, the temperature dependence of the specific heat ( $C_p$ ) was examined with a differential scanning calorimeter. Fig. 6 shows thermograms of the quasicrystal  $\text{Al}_{62}\text{Cr}_{21}\text{Si}_{17}$  alloy in as-quenched and annealed ( $680\text{ K} \times 1\text{ min}$ ) states, along with the data of the equilibrium  $\text{Al}_{13}\text{Cr}_4\text{Si}_4$  compound with a cubic structure obtained by annealing the as-quenched sample at 850 K for 1 h. The  $C_p$  value of the as-quenched quasicrystal is about  $22.5\text{ J mol}^{-1}\text{ K}^{-1}$  near room temperature. As the temperature rises, the  $C_p$  value increases gradually by the increase in the ease of thermal vibration of atoms, but the increase in  $C_p(T)$  becomes smaller at temperatures above about 460 K. Since no distinct change in X-ray diffraction pattern is observed before and after annealing at 600 K for 1 h, the difference in the  $C_p(T)$  values between the

as-quenched and the annealed samples, i.e., the occurrence of the irreversible broad exothermic peak, is believed to result from the heating-induced irreversible structural change probably due to the annihilation of various kinds of quenched-in ‘defects’ and a local rearrangement of the constituent atoms in the quasicrystal into a lower configuration energy state. Furthermore, it can be seen that the  $C_p$  values in the whole temperature range are consistently higher by about  $0.2$  to  $0.5\text{ J mol}^{-1}\text{ K}^{-1}$  for the as-quenched sample than for the stable cubic  $\text{Al}_{13}\text{Cr}_4\text{Si}_4$ . The decrease in  $C_p(T)$  is attributed to the structural change from the nonequilibrium quasicrystalline structure with higher atomic configuration energy to the equilibrium cubic structure with lower configuration energy. Fig. 6 also shows that the temperature dependence of vibrational specific heat is larger by about 8% for the quasicrystalline phase than for the cubic phase. Such a difference leads us to infer that the quasicrystal possesses a lower packing density as compared with the equilibrium cubic compound, being consistent with the previous experimental results [22, 23] that the density of Al–Mn quasicrystal increases by about 1.5% upon the structural change from the quasicrystal to the stable phase. The value of  $\Delta H_{i,\text{exo}}$  ( $\equiv \int_{400}^{680} \Delta C_p dT$ ) is estimated to be about  $431\text{ J mol}^{-1}$ , being smaller by about 15% than that ( $505\text{ J mol}^{-1}$ ) [24] for  $\text{Al}_{60}\text{Cr}_{15}\text{Si}_{25}$  amorphous alloy with a similar alloy component. This suggests that the quasicrystalline structure which has been thought [25] to possess a near-neighbour bond orientational order is in a considerably lower state of atomic configuration energy as compared with the amorphous structure.

### 3.3. Electrical resistivity

Fig. 7 shows the electrical resistivity of the quasicrystal  $\text{Al}_{62}\text{Cr}_{19}\text{Si}_{19}$  as a function of temperature. The resistivity shows a positive temperature dependence and increases with rising temperature from  $2.83\ \mu\Omega\text{m}$  at 4.2 K to  $3.65\ \mu\Omega\text{m}$  at 250 K. The resistivity ( $\rho$ ) as a function of temperature ( $T$ ) varies in the approximate relation of  $\rho \propto T$  over the wide temperature range except below about 50 K. The high resistivity combined with a slightly positive temperature dependence

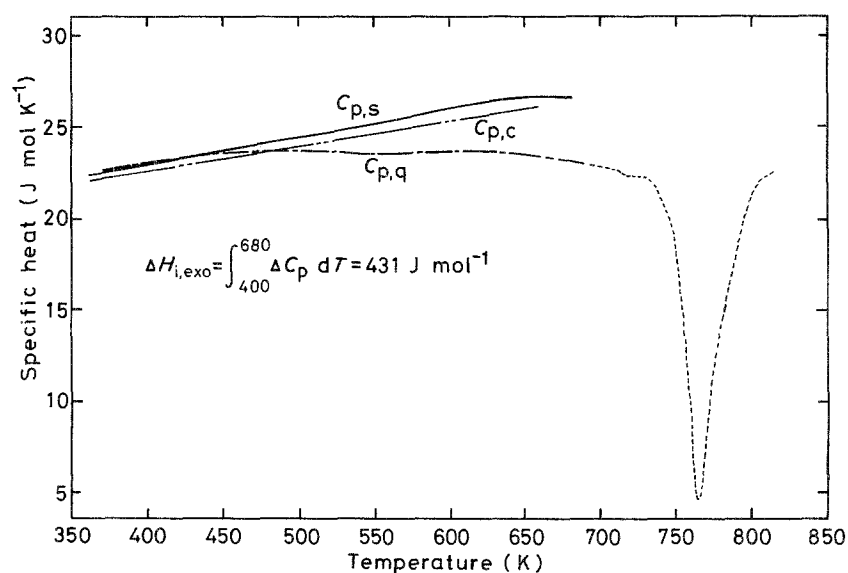


Figure 6 Thermogram of a quasicrystalline  $\text{Al}_{62}\text{Cr}_{21}\text{Si}_{17}$  alloy in as-quenched and annealed ( $680\text{ K} \times 1\text{ min}$ ) states ( $40\text{ K min}^{-1}$ ). The thermogram of a cubic  $\text{Al}_{13}\text{Cr}_4\text{Si}_4$  compound obtained by annealing the quasicrystalline phase at 850 K for 1 h was also presented for comparison.

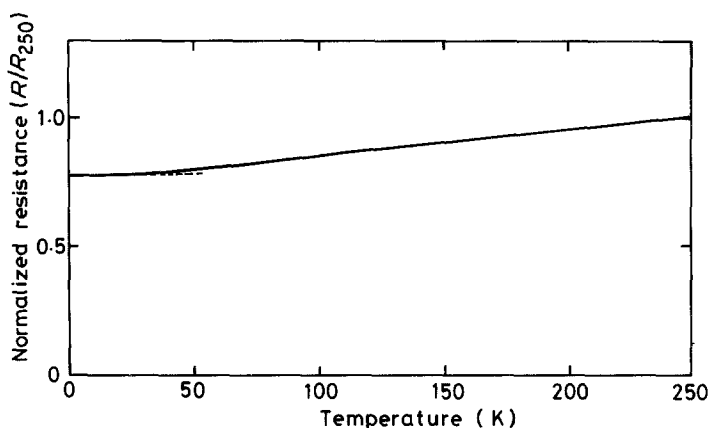


Figure 7 Change in the electrical resistivity of a rapidly quenched  $\text{Al}_{62}\text{Cr}_{19}\text{Si}_{19}$  alloy as a function of temperature.  $\rho_{250} = 3.65 \mu\Omega\text{m}$ .

for the Al–Cr–Si quasicrystal agrees with the results [5, 26] for Al–(Mn, V or Cr) quasicrystals without the silicon metalloid.

#### 4. Summary

The rapidly quenched structure of Al–Cr–Si alloys containing a large amount of silicon was examined and the quasicrystal was found to be formed in the vicinity of an alloy composition of  $\text{Al}_{62}\text{Cr}_{19}\text{Si}_{19}$ . The features of microstructure, thermal stability and electrical resistivity of the Al–Cr–Si quasicrystal are summarized as follows.

1. The quasicrystalline phase was determined to have a stoichiometric composition of  $\text{Al}_{13}\text{Cr}_4\text{Si}_4$  from the analytical composition data. The phase is composed of randomly-oriented equiaxed grains with a size of about  $0.5 \mu\text{m}$ .

2. The quasicrystal transforms to a stable cubic  $\text{Al}_{13}\text{Cr}_4\text{Si}_4$  compound in a narrow temperature range from 710 to 800 K accompanied by a transformation heat of  $2.57 \text{ kJ mol}^{-1}$ . The activation energy for the phase transformation was evaluated to be about  $85 \text{ kJ mol}^{-1}$ .

3. A broad exothermic reaction was found to occur during heating in the temperature range from 425 to the temperature just below the onset transformation temperature. The appearance of the low-temperature exothermic peak was interpreted as due to the structural change from a quenched-in high energy state to an annealing-induced lower energy state.

4. The electrical resistivity shows a positive temperature dependence and the variation occurs almost linearly at temperatures above about 50 K. The resistivities at 4.2 and 250 K are 2.83 and  $3.65 \mu\Omega\text{m}$ , respectively, and the temperature coefficient at 250 K is  $9.33 \times 10^{-4} \text{ K}^{-1}$ .

#### References

1. K. SCHECHTMAN, I. A. BLECH, D. GRATIAS and J. W. CAHN, *Phys. Rev. Lett.* **53** (1984) 1951.
2. D. SCHECHTMAN and I. A. BLECH, *Met. Trans.* **16A** (1985) 1005.
3. K. V. RAO, J. FILDER and H. S. CHEN, *Europhys. Lett.* **1** (1986) 647.
4. A. INOUE, L. ARNBERG, B. LEHTINEN, M. OGUCHI and T. MASUMOTO, *Met. Trans.* **17A** (1986) 1657.
5. A. INOUE, H. M. KIMURA and T. MASUMOTO, *J. Mater. Sci.* **22** (1987) 1758.
6. C. H. CHEN and H. S. CHEN, *Phys. Rev.* **B33** (1986) 2814.
7. P. RAMACHANDRARAO and G. V. S. SASTRY, *Pramana* **25** (1985) 225.
8. G. V. S. SASTRY, V. V. RAO, P. RAMACHANDRARAO and T. R. ANANTHARAMAN, *Scripta Met.* **20** (1986) 191.
9. N. K. MUKHOPADHYAY, G. N. SUBBANNA, S. RANGANATHAN and K. CHATTOPADHYAY, *ibid.* **20** (1986) 525.
10. Z. ZHANG, H. Q. YE and K. H. KUO, *Phil. Mag. A* **52** (1985) L49.
11. K. HIRAGA, M. HIRABAYASHI, A. INOUE and T. MASUMOTO, *J. Phys. Soc. Jpn* **54** (1985) 4077.
12. K. KIMURA, T. HASHIMOTO, K. SUZUKI, K. NAGAYAMA, H. INO and S. TAKEUCHI, *J. Phys. Soc. Jpn.* **55** (1986) 534.
13. H. A. DAVIES, *Amorphous Metallic Alloys*, edited by F. E. Lubrinsky (Butterworths, London, 1983), p. 8.
14. H. YOSHIDA, *Bull. Jpn Inst. Metals* **21** (1982) 925.
15. J. J. HREN, J. I. GOLDSTEIN and D. C. JOY (eds), *Introduction to Analytical Electron Microscopy* (Plenum, New York, 1979).
16. P. A. BANCEL, P. A. HEINEY, P. W. STEPHENS, A. I. GOLDMAN and P. M. HORN, *Phys. Rev. Lett.* **54** (1985) 2422.
17. K. HIRAGA, M. HIRABAYASHI, A. INOUE and T. MASUMOTO, *Sci. Rep. Res. Inst. Tohoku Univ.* **A32** (1985) 309.
18. T. MASUMOTO, A. INOUE, M. OGUCHI, K. FUKAMICHI, K. HIRAGA and M. HIRABAYASHI, *Trans. Jpn Inst. Metals* **27** (1986) 81.
19. A. INOUE, H. M. KIMURA and T. MASUMOTO, unpublished research, 1985.
20. H. E. KISSINGER, *Anal. Chem.* **29** (1957) 1702.
21. *Metals Databook*, (Japanese Institute of Metals, Maruzen, Tokyo, 1983), p. 24.
22. H. S. CHEN, C. H. CHEN, A. INOUE and J. T. KRAUSE, *Phys. Rev. B* **32** (1985) 1940.
23. K. F. KELTON and T. W. WU, *Appl. Phys. Lett.* **46** (1985) 1059.
24. A. INOUE, M. YAMAMOTO, H. M. KIMURA and T. MASUMOTO, unpublished research, 1986.
25. P. J. STEINHARDT, D. R. NELSON and M. RONCHETTI, *Phys. Rev. Lett.* **47** (1981) 1297.
26. K. FUKAMICHI, T. MASUMOTO, M. OGUCHI, A. INOUE, T. GOTO, T. SAKAKIBARA and S. TODO, *Metal Phys.* **16** (1986) 1059.

Received 14 July  
and accepted 22 September 1986